

Kinetics of color center formation in silica irradiated with swift heavy ions: Thresholding and formation efficiency

J. Manzano-Santamaría,^{1,2,a)} J. Olivares,^{1,3} A. Rivera,⁴ O. Peña-Rodríguez,⁴ and F. Agulló-López¹

¹Centro de Micro-Análisis de Materiales, Universidad Autónoma de Madrid (UAM), Cantoblanco, E-28049 Madrid, Spain

²Euratom/CIEMAT Fusion Association, Madrid, Spain

³Instituto de Óptica, Consejo Superior de Investigaciones Científicas (CSIC), C/Serrano 121, E-28006 Madrid, Spain

⁴Instituto de Fusión Nuclear, Universidad Politécnica de Madrid, C/José Gutiérrez Abascal 2, E-28006 Madrid, Spain

(Received 12 September 2012; accepted 24 September 2012; published online 8 October 2012)

We have determined the cross-section σ for color center generation under *single Br ion* impacts on amorphous SiO₂. The evolution of the cross-sections, $\sigma(E)$ and $\sigma(S_e)$, show an initial flat stage that we associate to atomic collision mechanisms. Above a *certain threshold* value ($S_e > 2$ keV/nm), roughly coinciding with that reported for the onset of macroscopic disorder (compaction), σ shows a marked increase due to electronic processes. In this regime, a *energetic cost* of around 7.5 keV is necessary to create a non bridging oxygen hole center-E' (NBOHC/E') pair, whatever the input energy. The data appear consistent with a non-radiative decay of self-trapped excitons. © 2012 American Institute of Physics. [<http://dx.doi.org/10.1063/1.4757886>]

The effects of swift heavy ion (SHI) beams on dielectric materials (electronic excitation regime) are the cumulative result (overlapping) of disorder tracks caused by individual ion impacts.^{1–5} In fact, the fluxes used in ion accelerators and other irradiation technologies imply that the time interval between successive ion impacts is much longer than the time needed to modify the atomic network of the material, around 10 ps. In other words, every impact only sees the “ashes” that remain after the previous impacts. Moreover, for SHI, the damaged region around the ion trajectory is only of a few nanometers, so that below $\sim 10^{12}$ cm^{−2}, the tracks are well isolated and can be individually registered.^{6,7} Therefore, the key problem is to understand the physical mechanisms operating at the nanoscale, during single ion impacts, which are responsible for structural modifications. This is very relevant in many technologies such as fission and fusion installations, the microelectronics and photonic industries, and the degradation of component and devices in space missions and hadron therapies using heavy ions.^{8–11}

So far, the microscopic mechanisms responsible for point defect generation inside the ion track in the electronic excitation regime remain to be elucidated and are still a matter of controversy. In principle, molecular dynamics simulations provide an efficient tool to follow the effects of a single ion impact.^{12,13} Unfortunately, those methods are not capable to deal with the quantum-mechanical formalism suitable to describe the excited electronic plasma. Therefore, phenomenological approaches, such as the thermal spike model,² are often used. They assume that the melting and re-solidification of the hot region around the trajectory are responsible for track formation. Although the thermal spike model has been satisfactorily used^{2,6,14–16} to account for a

number of relevant features of the observed damage in dielectrics, semiconductors, and even metals, it is becoming clear that the relaxation of the dense electronic excitation plays a very relevant role on the effects induced by SHI.¹¹ Therefore, these excitation effects should be more deeply investigated even at the phenomenological level. Moreover, a lot of attention has been paid to the defects and color centers generated by different types of irradiation but the microscopic mechanisms responsible for defect production under SHI irradiation have not been elucidated yet. In this Letter, we will address this problem for the case of silica, due to its fundamental and technological relevance.

When one fast ion traverses the material, a high density of *e-h* pairs are generated first, due to Coulomb interactions between the incoming ion and the electron system.¹⁷ The fast (ballistic) electrons or delta-electrons, mostly moving along a direction perpendicular to the ion trajectory, rapidly interact among themselves, and a thermal equilibrium is reached in times around 10 fs. Next, electron-phonon interaction sets in and promotes the energy transfer from the electron system to the atomic lattice. The final outcome, taking around 100–1000 fs, is the generation of a dense excitation spike (*e-h* pairs), coexisting in thermal pseudo-equilibrium with a thermal spike; being both bound to the ion trajectory. These two spikes are the initial ingredients needed to describe the later events associated to the relaxation of the electronic excitation, leading to either light emission or structural modifications and defect formation.¹⁸ Previous phenomenological models have focused on the exclusive effects of the thermal spike (phase transitions) whereas the effect of exciton relaxation on the atomic structure has been generally ignored. The role of the two spikes on the relative importance of the radiative and non-radiative processes is still unsolved and is a controversial issue, particularly referred to the dynamics of defect generation.

^{a)} Author to whom correspondence should be addressed. Electronic mail: javier.manzano@uam.es.

TABLE I. Main ion trajectory parameters obtained with SRIM 2008 (Refs. 43 and 44) for Bromine irradiations, where S_n max is 0.5 keV/nm.

E [MeV]	S_e (z=0) [keV/nm]	S_n (z=0) [keV/nm]	R_p [μ m]
2	1.0	0.09	1.3
5	2.1	0.06	2.9
10	3.4	0.05	4.5
15	4.7	0.04	5.8
25	5.7	0.03	7.6
40	7.2	0.02	9.4

Silica samples of 7×8 mm² and 1 mm thickness, provided by Momentive, have been irradiated at room temperature in the 5 MV tandem accelerator at the Centro de Microanálisis de Materiales (CMAM-UAM),¹⁹ with Br ions (mass number $A = 79$). The energies used as well as the projected ranges and the corresponding nuclear S_n and electronic S_e stopping powers are listed in Table I. Note that the choice of irradiations guarantees a rather constant collision deposition rate but a large span of electronic energy depositions. Ion currents were in the range 10–30 nA to avoid overheating of the samples. The evolution of most abundant color centers (NBOHC, E', and ODCs, Oxygen Deficient Centers) as a function of irradiation fluence has been monitored through their optical absorption spectra, both in the visible and UV range^{20,21} up to 8.2 eV, where the intrinsic absorption is already relevant. The main parameters used to fit the spectra are given in Table II; in addition to these bands, another one located at 7.3 eV and having a FWHM of 0.65 eV has been included for a proper fitting, following a recent work by Skuja.²²

A representative optical absorption spectrum of SHI-irradiated silica is shown in Fig. 1(a). The growth curves for all color centers as a function of fluence ϕ are Poisson-like,

$$N = N_S \{1 - \exp(-\sigma\phi)\}, \quad (1)$$

where N stands for the concentration per unit area, N_S is the saturation level, and σ an effective production cross-section. This behavior is exemplified in Fig. 1(b) for one of the irradiation energies (15 MeV). Similar average volume concentrations, $c = N/R_p$ (R_p is the projected range), up to around 10^{19} cm⁻³ are reached for all color centers in the surface layer limited by the projected range of the ions. These concentrations are much higher than those obtained under purely ionizing radiation like gamma rays ($\approx 10^{17}$ cm⁻³, not shown), confirming that new structural precursors are being created by the ion irradiation.^{23–25}

The initial growth rate, $\kappa = (dN/d\phi)_0$, derived from those coloring curves, provides the growth rate, $\kappa = \sigma N_S$, for

TABLE II. Main parameters used for the Gaussian deconvolution of the optical absorption spectra.^{20,21}

	NBOHC	ODC-II	E'	NBOHC	Extra Band	ODC-I
Position (eV)	4.8	5	5.8	6.8	7.3	7.6
FWHM (eV)	1–1.2	0.35–0.4	0.8–0.9	1.8	0.6	0.5
F	0.05	0.15	0.15	0.5	–	0.4

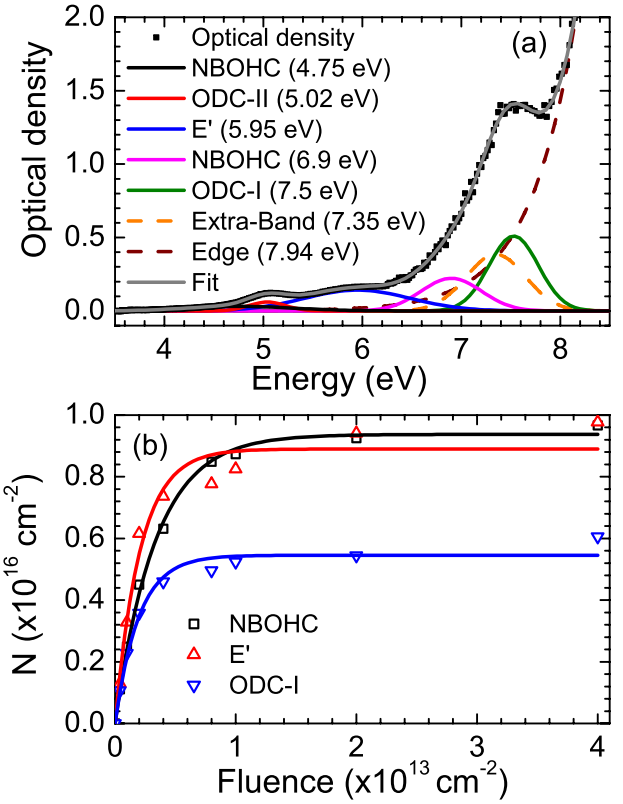
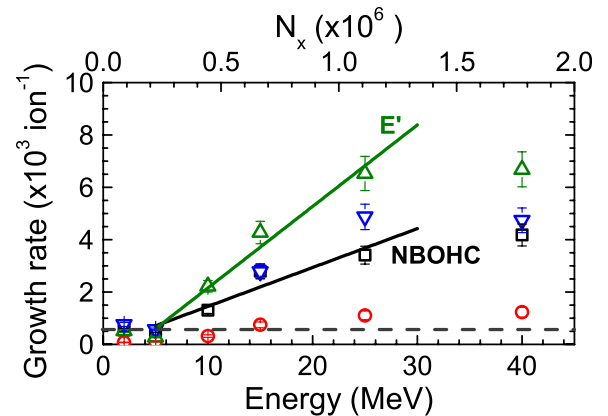


FIG. 1. (a) Gaussian deconvolution of a typical spectrum of irradiated silica and (b) kinetics for the overall density of the various color centers as a function of fluence. The fit to a Poisson law is depicted as solid lines. Both graphics correspond to an irradiation with Bromine at 15 MeV.

color center creation; i.e., the number of defects per single ion impact within the damage track. The data for κ as a function of the ion energy E and the electronic stopping power S_e are shown in Figures 2 and 3, respectively. Now, we will focus our attention on the NBOHC and E' centers because they have lower data dispersion than the ODC-I centers, which are possibly influenced by edge absorption. The curves show an initial flat stage at low energies (stopping powers) that can be attributed to atomic collision damage in accordance with the nuclear stopping power of the Br ions being essentially independent of energy (see Table I). Above

FIG. 2. Growth rate of color centers: NBOHC (\square), ODC-II (\circ), E' (\triangle), and ODC-I (∇) as a function of the total ion energy. Solid lines are drawn to visualize their evolution. Alternative abscissa scale is the overall e - h pair population per impact.

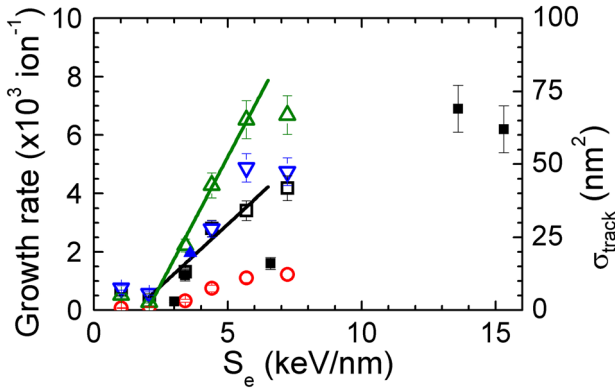


FIG. 3. Growth rate of color centers: NBOHC (\square), ODC-II (\circ), E' (\triangle), and ODC-I (∇) as a function of the electronic stopping power at the surface. Also is shown the area of the track for a single ion impact (\blacksquare and \blacktriangle were taken from the literature^{45,46}). Solid lines are a linear fit of the data. Alternative abscissa scale is the maximum temperature reached at the spike.

a certain energy *deposition threshold* (S_{th}) at the surface, κ experiences an approximately linear growth with the total ion energy E and with S_e , which should be associated to the relaxation of the electronic excitation. At higher energies and stopping powers, the linear rise bends down indicating that other competing processes may become operative. It is noteworthy that the threshold value for coloring obtained from Fig. 3 (around 2 keV/nm) has not been reported so far. It is in good accordance with that determined for the onset of network compaction as determined from ion-hammering and track etching experiments.^{26,27} Moreover, one observes that for the NBOHC and E' centers, κ shows quite similar evolution and even magnitude, suggesting that they may be mostly created as coupled pairs. The situation is quite similar to that found under F_2 excimer laser irradiation²⁸ as well as under above-edge synchrotron radiation.²⁹ From the linear dependence, κ vs. E , one obtains that the number of generated NBOHC/ E' pairs per MeV through electronic excitation is ≈ 130 , which implies an energetic cost of ≈ 7.5 keV per pair, independent of ion energy. For comparison, the collision mechanism generates around 600 pairs per Br impact.

In order to discuss the physical mechanisms for defect production and, particularly, the role of temperature, we have calculated the thermal and excitation spike profiles by using the Szenes analytical approximation.¹⁴ One considers that once reached thermal pseudo-equilibrium between the electron and phonon systems (before cooling), taken as initial time, $t=0$, the radial profiles for both spikes are Gaussian with the same width, $a_0 = 4.5$ nm

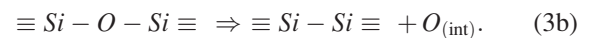
$$P(z, r, 0) = \frac{P(z, 0, 0)}{\pi a_0^2} \exp\left(-\frac{r^2}{a_0^2}\right), \quad (2)$$

where P is independent for, either, the exciton concentration, N_x , or the local temperature T . N_x represents the total number of generated $e-h$ pairs even if they do not form bound or self-trapped pairs.³⁰ The width a_0 can be related to the mean free path of the electrons as discussed by Toulemonde and coworkers,² using two coupled differential equations for electrons and heat (phonon) transport. The maximum temperature reached at the spike axis is $T_M = T(0, 0, 0)/(\pi a_0^2) = gS_e/(\pi a_0^2 \rho C)$, with a thermal efficiency ratio,

$g = 0.36$ (Ref. 31) and the physical parameters (density ρ and heat capacity C) reported for silica. Within this formalism, authors have described track generation as a compaction effect occurring above a certain temperature in the spike. Then, the increase in the area of the track with stopping power can be easily predicted. In view of a similar threshold obtained here for the coloring yield, one may try to correlate that yield κ with the cross-section (area) of the track (included in Fig. 3). The correlation is rather good, suggesting that a certain density of color centers ≈ 0.05 defects per nm^3 is generated inside the track cross-section. Anyhow, one still needs to understand which are the microscopic mechanisms leading to bond scission and, consequently, to point defect production. A thermal bond-breaking mechanism, such as that invoked for LiNbO_3 ,³ would predict a nonlinear increasing concentration of defects with input energy that does not agree with our experimental results.

As an alternative, let us now focus our attention on the correlated exciton spike as the source for the color centers. The possibility of exciton decay as the origin for defect production in oxides has been proposed and extensively discussed by Itoh and Stoneham³² and it is well established for halides. For SiO_2 , this mechanism appears strongly supported from some experimental works using irradiation with high energy electrons,^{32–34} synchrotron photon pulses,³⁵ and laser pulses,^{36,37} although not direct proof is yet available for the case of ion irradiation. Moreover, the non-radiative exciton decay as a mechanism for point defect production in silica and quartz has received strong support from a number of theoretical studies on exciton dynamics and relaxation.^{38,39} The total electron-hole density at z obtained by integration of expression (2) along r is usually written in the form: $N_x(z) = S_e(z)/I$,^{40,41} where I is an effective ionization energy and $I \approx 3 E_G$ (gap energy). For silica ($E_G \approx 8$ eV), integration along the whole trajectory yields $N_x \approx E$ (eV)/25. For the energies used in our irradiations, this electron-hole density becomes close to the atomic density of the material, suggesting the formation of dense electron-hole plasma. To facilitate comparison, we have included as an additional abscissa axis the total electro-hole density in Fig. 2. It comes out from the figure that the relation κ vs N_x is approximately linear, indicating that the color center yield per excited $e-h$ pair is roughly constant, independently of the ion type and energy. A relative constant efficiency of $\approx 0.1\%$ of the total $e-h$ population is obtained for the conversion of pairs into color centers, regardless of the temperature reached in the spike. This yield, which refers to exciton formation and self-trapping aside from defect formation, is not far from that found for ion irradiation of alkali halides where the exciton model is well established.⁴²

Specific mechanisms that have been proposed^{28,29,36,37} for the processes of exciton relaxation in SiO_2 are



The first one becomes operative after one-photon absorption of F_2 excimer laser light has a quantum efficiency of 3×10^{-4} and accounts for the similar concentrations of NBOHC and

E' centers. Note that this efficiency is not very different from that found in our experiments. On the other hand, reaction (3b), leading to Frenkel pairs, explains the formation of the ODCs. Our data indicate that, under ion irradiation, both channels operate in parallel and could be derived from a common exciton recombination event. A remarkable finding by Hosono *et al.*²⁸ is that the recombination giving rise to Eq. (3b) preferentially occurs at heavily strained bonds, which correspond mostly to three- and four-membered rings. The possibility that the threshold for color center formation found in this work may be due to the bond straining associated to compaction by irradiation would account for the coincidence between both thresholds and should be investigated in further works. This may reveal the connection between the macroscopic and microscopic effects of irradiation.

In summary, the data offered in this work suggest that electronic excitation plays an important role in the generation of point defects in silica under SHI irradiation. In view of the available theoretical and experimental information, one may safely propose that the color centers are generated by non-radiative decay of self-trapped excitons and that no energy barrier has to be overcome to generate the defects. A threshold stopping power for color center generation has been obtained and approximately coincides with that previously found for network compaction. The details of such process should deserve further experimental and theoretical work to become fully understood. Approximated values for the energetic yield of the electronic processes have been calculated, providing relevant information for scientists and engineers dealing with ion-beam damage to materials.

This work has been supported by Spanish Ministry MICINN through the Project MAT2011-28379-C03-02 and by Madrid Community through the Project TECHNOFUSION (S2009/ENE-1679). O.P.R. would like to thank Moncloa Campus of International Excellence (UCM-UPM) foundation for offering a PICATA postdoctoral fellowship. Dedicated to the memory of Dr. Marshall Stoneham (deceased).

¹R. L. Fleischer, P. B. Price, and R. M. Walker, *Nuclear Tracks in Solids: Principles and Applications* (University of California Press, Berkeley, 1975).

²M. Toulemonde, W. Assmann, C. Dufour, A. Meftah, F. Studer, and C. Trautmann, in *Ion Beam Science: Solved and Unsolved Problems*, edited by P. Sigmund (Royal Danish Academy of Sciences and Letters, Copenhagen, 2006), pp. 263–291.

³F. Agulló-López, G. García, and J. Olivares, *J. Appl. Phys.* **97**, 093514 (2005).

⁴N. Itoh, D. M. Duffy, S. Khakshouri, and A. M. Stoneham, *J. Phys.: Condens. Matter* **21**, 474205 (2009).

⁵A. Rivera, M. L. Crespo, J. Olivares, G. García, and F. Agulló-López, *Nucl. Instrum. Methods B* **268**, 2249 (2010).

⁶A. Meftah, F. Brisard, J. M. Costantini, E. Dooryhee, M. Hage-Ali, M. Hervieu, J. P. Stoquert, F. Studer, and M. Toulemonde, *Phys. Rev. B* **49**, 12457 (1994).

⁷P. Kluth, C. S. Schnorr, O. H. Pakarinen, F. Djurabekova, D. J. Sprouster, R. Giuliani, M. C. Ridgway, A. P. Byrne, C. Trautmann, D. J. Cookson, K. Nordlund, and M. Toulemonde, *Phys. Rev. Lett.* **101**, 175503 (2008).

⁸*Handbook of Ion Implantation Technology*, edited by J. F. Ziegler, 1st ed. (North Holland, Amsterdam, 1992).

⁹E. R. Hodgson, *J. Nucl. Mater.* **258–263**, 226 (1998).

¹⁰P. D. Townsend, P. J. Chandler, and L. Zhang, *Optical Effects of Ion Implantation* (Cambridge University Press, Cambridge, UK, 1994).

¹¹A. Rivera, J. Olivares, G. García, J. M. Cabrera, F. Agulló-López, and F. Agulló-López, *Phys. Status Solidi A* **206**, 1109 (2009).

¹²K. Nordlund, M. Ghaly, R. S. Averback, M. Caturla, T. Diaz de la Rubia, and J. Tarus, *Phys. Rev. B* **57**, 7556 (1998).

¹³F. Mota, M.-J. Caturla, J. M. Perlado, A. Ibarra, M. León, and J. Mollá, *J. Nucl. Mater.* **367–370**, 344 (2007).

¹⁴G. Szenes, *Phys. Rev. B* **60**, 3140 (1999).

¹⁵A. Kamarou, W. Wesch, E. Wendler, A. Undisz, and M. Rettenmayr, *Phys. Rev. B* **73**, 184107 (2006).

¹⁶K. Awazu, S. Ishii, K. Shima, S. Roorda, and J. L. Brebner, *Phys. Rev. B* **62**, 3689 (2000).

¹⁷M. Nastasi, J. Mayer, and J. K. Hirvonen, *Ion-Solid Interactions: Fundamentals and Applications* (Cambridge University Press, 1996).

¹⁸A. Rivera, A. Méndez, G. García, J. Olivares, J. M. Cabrera, and F. Agulló-López, *J. Lumin.* **128**, 703 (2008).

¹⁹See <http://www.cmam.uam.es/> for CMAM—Centre for Micro Analysis of Materials (2011).

²⁰*Defects in SiO₂ and Related Dielectrics*, edited by G. Pacchioni, L. Skuja, and D. L. Griscom, 1st ed. (Springer, Dordrecht, 2000).

²¹L. Skuja, M. Hirano, H. Hosono, and K. Kajihara, *Phys. Status Solidi C* **2**, 15 (2005).

²²L. Skuja, K. Kajihara, M. Hirano, and H. Hosono, *Phys. Rev. B* **84**, 205206 (2011).

²³D. L. Griscom, M. E. Gingerich, and E. J. Friebele, *Phys. Rev. Lett.* **71**, 1019 (1993).

²⁴H. Imai, K. Arai, J. Isoya, H. Hosono, Y. Abe, and H. Imagawa, *Phys. Rev. B* **48**, 3116 (1993).

²⁵H. Hosono, M. Mizuguchi, H. Kawazoe, and T. Ogawa, *Appl. Phys. Lett.* **74**, 2755 (1999).

²⁶S. Klaumünzer, *Nucl. Instrum. Methods B* **225**, 136 (2004).

²⁷J. Jensen, A. Razpet, M. Skupinski, and G. Possnert, *Nucl. Instrum. Methods B* **243**, 119 (2006).

²⁸H. Hosono, Y. Ikuta, T. Kinoshita, K. Kajihara, and M. Hirano, *Phys. Rev. Lett.* **87**, 175501 (2001).

²⁹F. Messina, L. Vaccaro, and M. Cannas, *Phys. Rev. B* **81**, 035212 (2010).

³⁰A. N. Trukhin, *J. Non-Cryst. Solids* **149**, 32 (1992).

³¹G. Szenes, *Nucl. Instrum. Methods B* **122**, 530 (1997).

³²N. Itoh and M. Stoneham, *Materials Modification by Electronic Excitation* (Cambridge University Press, 2000).

³³N. Itoh, T. Shimizu-Iwayama, and T. Fujita, *J. Non-Cryst. Solids* **179**, 194 (1994).

³⁴H. Hosono, H. Kawazoe, and N. Matsunami, *Phys. Rev. Lett.* **80**, 317 (1998).

³⁵K. Kajihara, M. Hirano, L. Skuja, and H. Hosono, *Phys. Rev. B* **78**, 094201 (2008).

³⁶T. E. Tsai and D. L. Griscom, *Phys. Rev. Lett.* **67**, 2517 (1991).

³⁷Y. Ikuta, S. Kikugawa, M. Hirano, and H. Hosono, *J. Vac. Sci. Technol. B* **18**, 2891 (2000).

³⁸S. Ismail-Beigi and S. G. Louie, *Phys. Rev. Lett.* **95**, 156401 (2005).

³⁹R. M. Van Ginoven, H. Jónsson, and L. R. Corrales, *J. Non-Cryst. Solids* **352**, 2589 (2006).

⁴⁰R. C. Hughes, *Appl. Phys. Lett.* **26**, 436 (1975).

⁴¹R. C. Hughes, *Phys. Rev. Lett.* **30**, 1333 (1973).

⁴²A. Rivera, J. Olivares, G. García, and F. Agulló-López, *J. Phys.: Condens. Matter* **24**, 085401 (2012).

⁴³J. Ziegler, "SRIM—The stopping and range of ions in matter," <http://www.srim.org/> (2008).

⁴⁴J. F. Ziegler, *The Stopping and Range of Ions in Solids* (Pergamon, 1985).

⁴⁵C. C. Stanescu, "SiO₂ Sur Silicium: Comportement Sous Irradiation Avec Des Ions Lourds," Ph.D. dissertation, University of Caen/Basse-Normandie, 2002.

⁴⁶O. Peña-Rodríguez, J. Manzano-Santamaría, J. Olivares, A. Rivera, and F. Agulló-López, *Nucl. Instrum. Methods B* **277**, 126 (2012).